Fifth International Symposium on Marine Propulsors
smp'17, Espoo, Finland, June 2017

Design Optimization of a Horizontal Axis Tidal Stream Turbine Blade Using CFD

Madhan Kumar[1], Gwon Woo Nam[2], Seung Jin Oh[2], Jeonghwa Seo[3], Abdus Samad[1], Shin Hyung Rhee[2,3]

[1]Department of Ocean Engineering, Indian Institute of Technology Madras, Chennai, India
[2]Department of Naval Architecture and Ocean Engineering, Seoul National University, Seoul, Republic of Korea
[2]Research Institute of Marine Systems Engineering, Seoul National University, Seoul, Republic of Korea

ABSTRACT

This article presents a design and optimization approach for a horizontal axis tidal stream turbine, through a surrogate-based optimization technique and numerical simulation using SNUFOAM, which is a computational fluid dynamics (CFD) code based on OpenFOAM toolkit. By using the method, design of a scaled model of a 100 kW class horizontal axis tidal stream turbine was optimized to maximize energy extracting performance. Several designs were produced through the three-level full factorial sampling technique, evaluated using the CFD code to find the objective function**,** the power coefficient. The Kriging surrogate was constructed for optimization, of which design variables were blade thickness parameters. For numerical simulation, grid dependency tests were conducted and the optimal number of cells was found to be around 0.5 million. A moving reference frame method was used to enable turbine rotation. Through this approach, the power coefficient of the turbine was increased by 18%.

Keywords

Computational fluid dynamics, design optimization, tidal stream turbine, SNUFOAM

1 INTRODUCTION

The renewable energy harvesting efforts from ocean environments have grown. Tidal stream turbines utilize tide, which is easy to predict its direction and magnitude and the energy density is higher than that of the wind. Among those, a horizontal axis tidal stream turbine (HATST), which has high energy extracting capability, is widely used (Douglas et al., 2008).

Albeit the HATST has its origin in wind turbines, it is significantly different from them in certain characteristics such as fluid medium, loading, corrosion, and cavitation, etc. Batten et al. (2006) investigated the influence of various hydrodynamic parameters on the performance of marine current turbines. They also discussed the effect of pitch angle and camber on the cavitation characteristics of the turbine. O'Doherty et al. (2009) presented the validation of numerical analysis with experimental results and concluded that the Reynolds stress model predicted more accurate power coefficient (C_P) results than other turbulence models. Harrison et al. (2010) compared numerical simulations and experimental results of far wake of horizontal axis tidal turbines. The thrust coefficient (C_T) and ambient turbulence levels were found to be the main factors that influence the wake. Lawson et al. (2011) evaluated the effects of unstructured grid and computational time step size on HATST analysis. They showed that the grid generation was the major factor in the accuracy of the numerical analysis in designed operation conditions, whereas the time step size had no significant effect on transient analysis. Song et al. (2012) performed numerical and experimental investigations on various configurations of 100 kW HATSTs and concluded that the modified blade with tip rake provides maximum efficiency and improved cavitation characteristics. Lee et al. (2012) discussed the computational analysis of various configurations of HATST using the blade element momentum theory and CFD analysis. A significant agreement between those results was reported. Park et al. (2016) recently reported their study on HATST performance in off-design conditions.

As HATST works in various conditions, a design optimization method is required to maximize the turbine efficiency in various operating conditions. Surrogate models are suitable for optimization of these

problems, by minimizing number of computations. In a large design space, they guess the response in the unsampled regions (Goel et al., 2007). There are various surrogates such as Kriging, polynomial regression models, artificial neural networks etc.

Each of them has their own merits and demerits. In this work, the Kriging model was chosen because it suits well for low dimensionality problems (Díaz-Manríquez et al., 2011). The Kriging model or Kriging surrogate model was developed by Danie Krige, in geostatistics, and later improved by Matheron (1963). Sacks et al. (1989) employed the Kriging model to estimate the deterministic computer codes. Kriging model imitates a relationship between the objective function and the design variable. It employs the Gaussian random process to approximate the given function (Jeong et al., 2012). The Kriging model was applied to the aerospike nozzle (Simpson et al., 2001), low pressure turbine exhaust hood (Wang et al., 2010), aeroengine turbine disc (Huang et al., 2011), and cooling turbine blade (Ao et al., 2012) for design optimization. Samad et al. (2008) performed optimization of the axial compressor blade by weighted average surrogates with Kriging and other surrogate models. A similar approach was successfully applied to a wave energy device recently (Halder et al., 2017).

The expertise obtained from the optimization of wind turbines can be extended to the optimization of tidal stream turbines. The parameters such as rotor diameter, chord, twist, and thickness can be used as design variables, whereas the lift and drag coefficient can be taken as the objective functions for the aerodynamic optimization (Fuglsang et al., 1999). Tahani et al. (2015) performed multi-objective optimization on contra-rotating horizontal axis tidal turbines. Maximizations of torque and C_P were taken as the objective with the design variables chord and twist distributions along the blade span. Torque and C_P were improved by 4.3% and 57.9%, respectively. Huang et al. (2015) also optimized a contra-rotating tidal turbine with blade pitch angle as the design variable, and maximization of C_P and torque coefficient as objective. Carrasco et al. (2016) optimized wind turbine blade to improve power production by using Kriging models. Genetic algorithm (GA) and sequential quadratic programming (SQP) methods were used for global and local search respectively.

In this work, an optimization of a HATST combined with CFD analyses is reported and the fluid dynamic characteristics of the optimized turbine are discussed. A single-objective optimization to maximize C_P by modifying the maximum thickness (MT) and the maximum thickness location (MTL) has been done. The Kriging surrogate-based optimization method was used with CFD simulations and description showing the fluid dynamics behind the performance improvement was reported in this paper.

2 TEST MODEL AND DESIGN VARIATIONS

2.1. Description of the reference model and the test condition

A 1/20th scale model of a 100 kW-class HATST (see Figure 1), which was used in the experiments of Seo et al (2016) was selected as the reference design. The radius (R) of the turbine was 200 mm. It is a three-bladed HATST with the blade section of NACA 63-418. The chord length of the blade at 0.3*R* was 34.2 mm. The turbine rotates in clockwise direction when viewed from the upstream side. For simplicity, the tower and nacelle of the HATST was not included in the computational study.

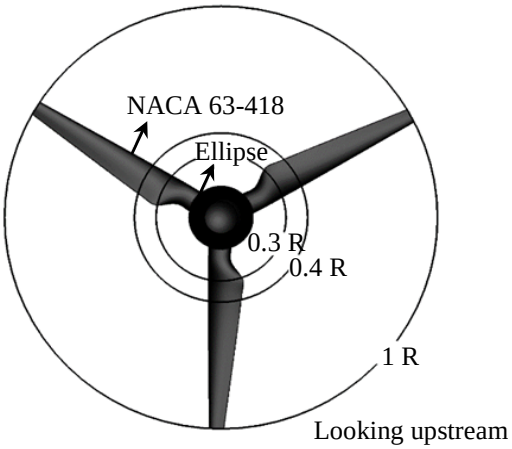

Figure 1. Geometry of the HATST (Seo et al., 2016)

In this study, three tip-speed-ratio (TSR) conditions were selected following the experimental study (Seo et al., 2016). Table 1 shows the test conditions. The turbine revolution rate was fixed at 240 rpm while the flow speed was varied to achieve the required TSR.

Table 1. Test conditions

TSR	Turbine speed (rpm)	Fluid velocity (m/s)	Reynolds number (Re) at 0.4R
3.3	240	1.523	60,000
3.5		1.436	58,000
4.0		1.257	53,000

2.2. Optimization methodology

There are ample parameters to modify a turbine blade so that a higher power extraction capability can be obtained. To optimize it, initially, the objective function (C_P) and the design variables (MT and MTL) are defined, following a parametric study on airfoil design by Ma et al. (2015). After that, the optimization approach given in Figure 2 is followed. The

optimization methodology is explained briefly in the section below.

2.2.1. *Selection of experimental design*

NACA 63-418 has MT of 18% chord length (C) and MTL at 33.9% C from the leading edge. For optimization, the sampling was done using 3^2 factorial design technique (see Figure 3), 3^2 factorial design consists of two design variables at every three levels. The coordinate (0, 0) denotes the reference blade and (+20, -20) represents the blade with a 20% increase in MT and MTL decreased by 20% from the reference profile, i.e. MT 21.6% C and MTL 27.1% C.

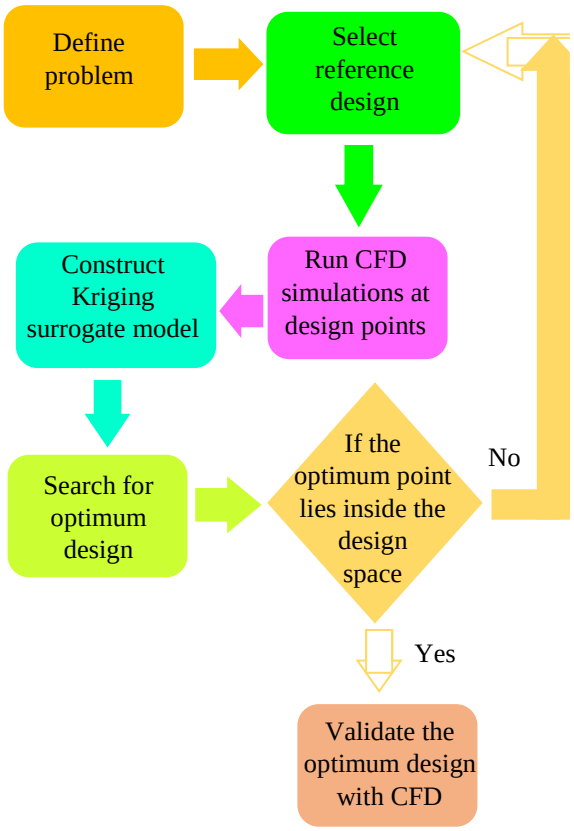

Figure 2. Flowchart of optimization methodology

Table 2 shows the limits of design variables which were selected after a few iterations in the optimization loop described in Figure 2.

Table 2. Limits of design variables

Variables	Lower limit	Upper limit
MT	-20%	+40%
MTL	-40%	+40%

The hydrofoil profile modification was done by Qblade, open source software for design and analysis of wind turbines (Marten et al., 2013). The coordinates of the modified hydrofoil profiles were used to build three-dimensional (3D) geometries. The modified profiles with the reference one is shown in Figure 4.

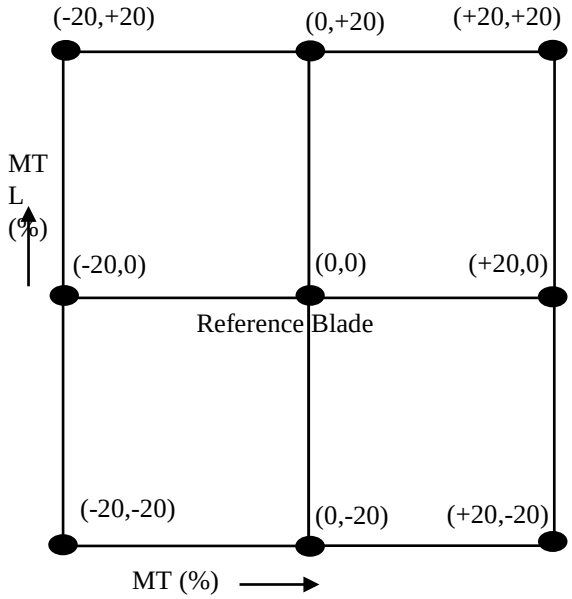

Figure 3. Schematic of 3^2 factorial method

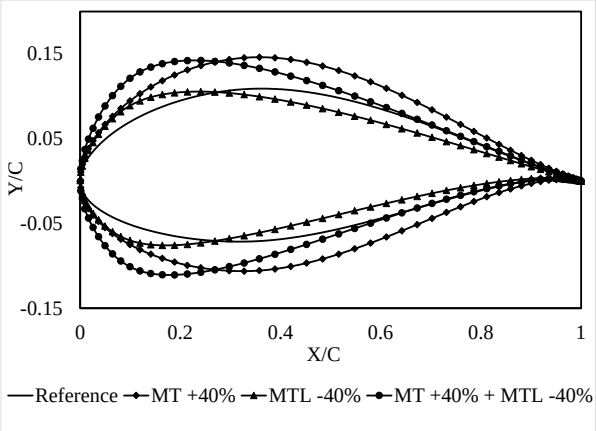

Figure 4. Reference and modified hydrofoil profiles

2.2.2 *Kriging surrogate model*

The Kriging model is a statistical interpolator technique to fit the design points to predict the objective function values in a design space. It can be given as

$$y(x)=g(x)+Z(x) \quad (1)$$

where, y(x) is the Kriging surrogate, g(x) is the polynomial function of the known design points and Z(x) is the stochastic function based on Gaussian distribution with zero mean and variance σ^2. The covariance matrix is given by

$$Cov[Z(x_a),Z(x_b)]= \sigma^2 R[R(x_a,x_b)]; a, b=1..n_s \quad (2)$$

where n_s is the number of sampling points, R is the symmetric correlation matrix of order (n_s*n_s) and diagonal values as unity, R (x_a, x_b) is the spatial correlation of the function between sample points x_a and x_b. The design points were evaluated by the CFD solver. The MATLAB toolbox DACE was used for the Kriging formulation (Lophaven et al., 2002).

2.2.3. *Optimal point search*

To obtain the optimal design point, SQP in *fmincon* function in MATLAB is used. It is an adoption of Newton method for constrained optimization (Boggs et al 1995) and approximates the objective and constraints as quadratic and linear functions respectively.

The execution of SQP involves the following steps, updating Hessian matrix, solving quadratic programming and performing line search and merit function calculation (Raza and Kim, 2008).The optimal point is validated with CFD simulation and error analysis is done to check to see if the surrogate prediction is correct.

3. COMPUTATIONAL METHODS

3.1. Governing equations and numerical models

The CFD code used in this study was SNUFOAM, a specialized code for naval hydrodynamics applications, based on OpenFOAM. A moving reference frame (MRF) was employed to realize the turbine rotation, without physically rotating the domain.

$$\nabla.(\overrightarrow{u_R}\otimes\overrightarrow{u_I}) + \overrightarrow{\Omega}\otimes\overrightarrow{u_I} = -\nabla\left(\frac{p}{\rho}\right) + v\nabla.\nabla(\overrightarrow{u_I}) \quad (3)$$

$$\nabla.\overrightarrow{u_R}=0 \quad (4)$$

Equations 3 and 4 represent the governing equations of the CFD solver: the Navier-Stokes equations with Coriolis force and the continuity equation. The flux corresponding to the rotation of the reference frame was calculated by the relative velocity and applied to the entire flow field for steady state analysis. A second order scheme and PIMPLE algorithm were chosen for spatial discretization and pressure-velocity coupling, respectively, and k-Ω SST was used as the turbulence model (Park et al., 2013). PIMPLE algorithm is a combination of PISO (Pressure implicit split operator) and SIMPLEC (Semi implicit method for pressure linked equations) algorithms

First, the computational domain for a single turbine blade was designed (see Figure 5). Dirichlet and Neumann boundary conditions were applied to the inlet and the outlet, respectively. In the periphery of the blade, interface boundary conditions using non-matching interface was used. No-slip boundary condition was applied to the blade surface, and slip wall condition was employed to the inner wall and outer wall boundary.

Considering the symmetry of the turbine, a fan-shaped block with a central angle of 120º was created, and the cyclic interface boundary condition was applied to the sides of the computational domain. Following Bahaj et al. (2007), the torque on the blade and drag force or negative thrust are expressed as C_P and C_T as shown in equations (5) and (6), respectively.

$$C_P = Q\,\omega\ / 0.5\rho V_A^3 S \quad (5)$$

$$C_T = T / 0.5\rho V_A^2 S \quad (6)$$

where, Q is torque on the blade, ω is angular velocity, ρ is density of water, S is turbine disk area, V_A is velocity of the tide, and T is negative thrust.

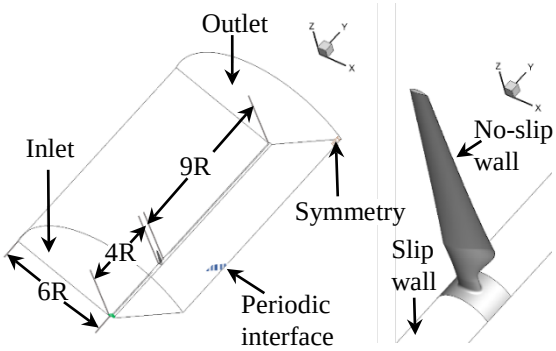

Figure 5. Computational domain with boundary conditions

3.2. Mesh generation

The computational domain was meshed with structured hexahedral cells, as they provide more stable and accurate solutions than the unstructured grids in general. Hence, an advanced meshing tool, SNUFOAM ShipMesh Advanced based on cfMesh was used for hexahedral Cartesian grid generation. To include the sharp trailing edge of the turbine, each turbine surface was divided and the surface feature was improved through split – rename – merge process. Additionally, a prism layer zone was applied around the blade surface to increase the grid resolution at the boundary layer.

4. RESULTS AND DISCUSSIONS

4.1. Grid dependency tests and validation

Table 3 shows the grid dependency test results for single blade domain. The grid resolution was varied in three different grids, which were used for TSR = 3.5 conditions. The fine and medium grids produced torque coefficients that are less than 10% different from the experimental results. Also, the difference between fine and medium grid results is less than 1%. Hence, the medium grid was selected for all the remaining runs.

Figure 6 shows the validation of CFD results with the experimental data (Seo et al., 2016). The experimental fluid dynamics (EFD) and the CFD results show the

same trend. CFD predicted C_T and C_P with error less than 2.15%. The C_P and C_T with variations of TSR were validated against the experimental results.

Table 3. Grid dependency test results

	Total cell count	Wall y+	C_P	C_T
Coarse	179,467	17.1	0.234	0.525
Medium	538,935	12.13	0.262	0.551
Fine	1,239,747	10.07	0.260	0.548

At TSR = 3.5, C_P was the highest and showed the best energy conversion performance. At high TSR, C_P decreased gradually as the angle of attack onto the turbine blade reduced.

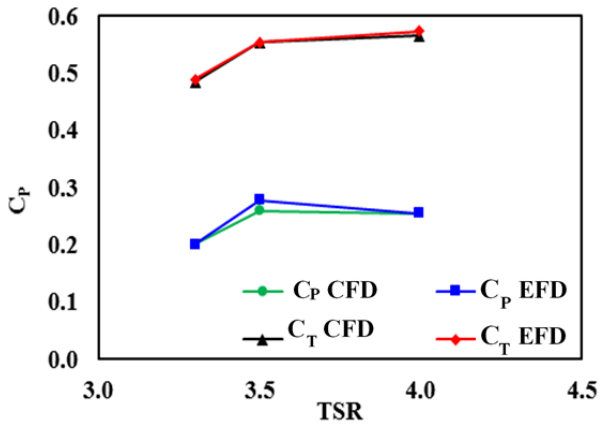

Figure 6. Comparisons of C_P and C_T from experiments and CFD analyses.

4.2. Optimization results

The response surface using the Kriging model was plotted with the normalized values of MT and MLT (see Figure 7). The optimal design was obtained by MT increased by 27.2% and MTL moved 29.8% towards the leading edge relative to the reference profile, i.e., MT 22.9% C and MTL 23.8 % C.

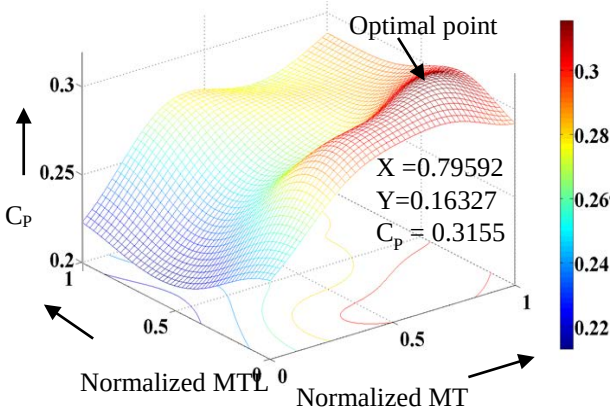

Figure 7. Response surface of Kriging model

Table 4 presents C_P for the optimal design predicted by Kriging and CFD. The surrogate model-produced result was accurate with only 2.13% error, compared to the CFD results. The optimal turbine produced 18% higher C_P than the reference case.

Figure 8 displays comparison of C_P for the reference and the optimum design. The optimum blade provided improved C_P at all TSR's. The changes in C_P with different TSR also reduced.

Table 4. Comparison of CFD Kriging model results

	MT (%)	MTL (%)	C_P (CFD)	C_P (Kriging)	Error (%)
Reference	0	0	0.262	-	
Optimal design	27.2	-29.8	0.3089	0.3155	2.13

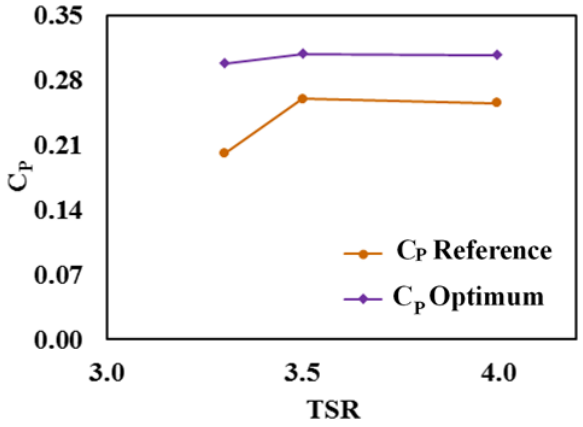

Figure 8. Comparisons of C_P for reference and optimum design.

4.3. Flow details of optimized design

The energy extracting mechanism is investigated through flow physics. In this study, pressure coefficient, turbulence kinetic energy, and tip vortex strength are examined. Figure 9 displays the pressure coefficient contours (C_{press}) on the turbine blade. Especially low-pressure region on the suction side was noticeable in the optimal case.

Figure 10 shows the turbulence kinetic energy distribution around the blade sections. The turbulence kinetic energy is concentrated at the suction side, where strong adverse pressure gradient exists. The turbulence kinetic energy increases along the radial direction, owing to 3D effects on the turbine blade. In the optimal design, the turbulence kinetic energy decreases dramatically. The reduced turbulence kinetic energy implies that the energy loss by the turbulence generation decreased in this optimal design case.

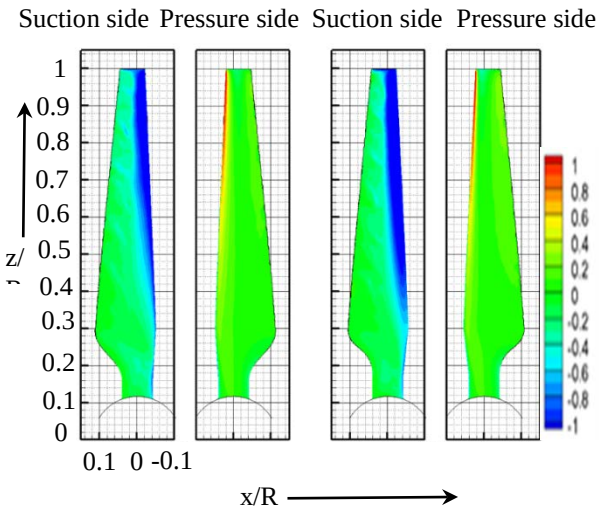

Figure 9. Pressure coefficient contours of the reference (left) and the optimum case (right)

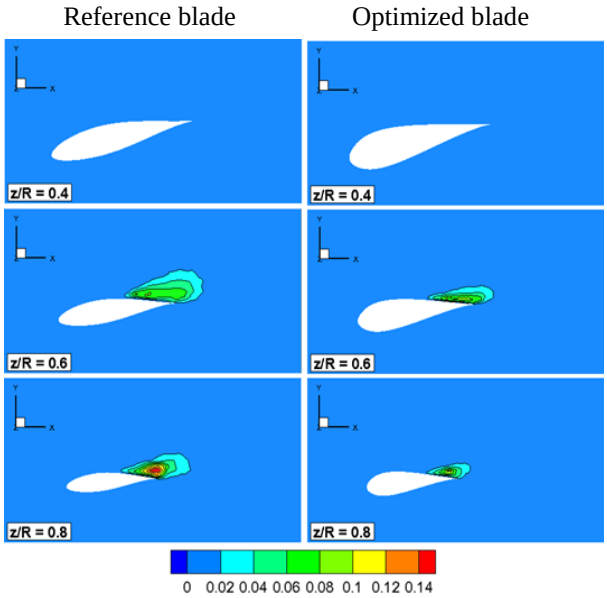

Figure 10. Turbulence kinetic energy contours at various cross-sections

Figure 11 shows the vorticity magnitude around the tip vortex region. The tip vortex increases in the optimized turbine case, as the pressure difference between the two sides increases, as shown in Figure 9. The tip vortex dissipates in the near wake, as reported in previous CFD studies (Harrison et al., 2010).

5. CONCLUSIONS

Design optimization of horizontal axis tidal stream turbine with computational fluid dynamics and Kriging surrogate models is presented. The conclusions are as follows.

- The Kriging model predicted the optimized design with commendable accuracy.
- The hydrofoil profile with a 27.2% increase in maximum thickness and 29.8% decrease in the maximum thickness location from the reference profile is found to be optimal. It improved the power coefficient by 18%.
- The enhanced power coefficient of the optimized blade can be attributed to the suppression of turbulence kinetic energy compared to that of the reference blade case.
- The optimized blade shows a high vorticity at blade tip compared to the reference one due to the high pressure difference across its suction and pressure side at tip region of blade.

As this study is limited to single objective optimization of power coefficient without considering any constraints, it is recommended to make the optimization method more realistic with multiple objective functions.

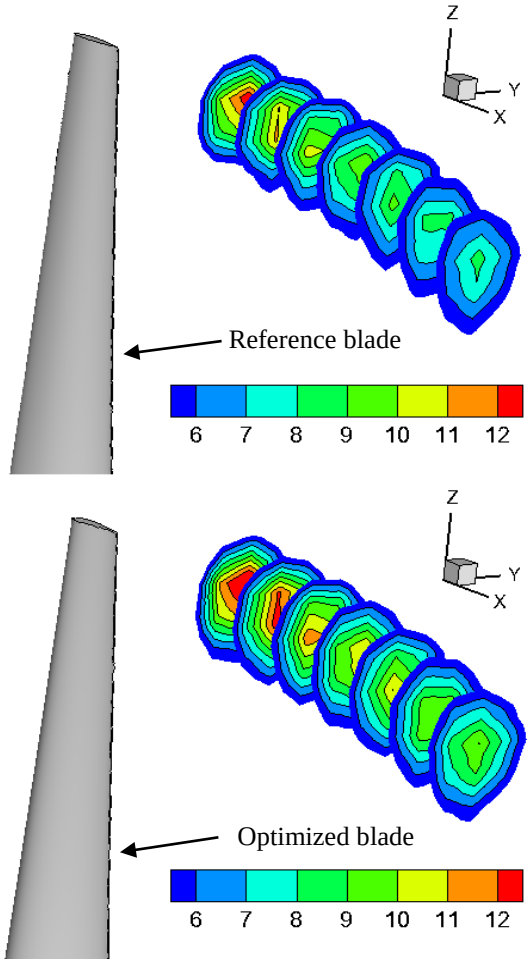

Figure 11. Vorticity magnitude at the tip vortex region (0.2 ≦x/R ≦ 0.5)

REFERENCES

Ao, L. B., Li, L., Li, Y. S., Wen, Z. X., & Yue, Z. F. (2012). 'Multi-objective design optimization of cooling turbine blade based on kriging model'. Applied Mechanics and Materials **184**, pp. 316–319.

Bahaj, A. S., Batten, W. M. J., & McCann, G. (2007). 'Experimental verifications of numerical predictions for the hydrodynamic performance of

horizontal axis marine current turbines'. Renewable Energy **32**(15), pp. 2479-2490.

Batten, W. M. J., Bahaj, A. S., Molland, A. F., & Chaplin, J. R. (2006). 'Hydrodynamics of marine current turbines'. Renewable energy **31**(2), pp. 249-256.

Boggs PT, Tolle JW (1995), 'Sequential quadratic programming'. Acta Numerica **4**(1), pp. 1–51.

Carrasco, A. D. V., Valles-Rosales, D. J., Mendez, L. C., & Rodriguez, M. I. (2016). 'A site-specific design of a fixed-pitch fixed-speed wind turbine blade for energy optimization using surrogate models'. Renewable Energy **88**, pp. 112-119.

Diaz-Manriquez A, Toscano-Pulido G and Gomez-Flores W. (2011, June 5-8). 'On the selection of surrogate models in evolutionary optimization algorithms', Proceeding of Evolutionary Computation (CEC), New Orleans, LA, USA,IEEE Congress, pp. 2155–2162.

Douglas, C. A., Harrison, G. P., & Chick, J. P. (2008). 'Life cycle assessment of the seagen marine current turbine'. Proceedings of the Institution of Mechanical Engineers, Part M: Journal of Engineering for the Maritime Environment **222**(1), pp. 1-12.

Fuglsang, P., & Madsen, H. A. (1999). 'Optimization method for wind turbine rotors'. Journal of Wind Engineering and Industrial Aerodynamics **80**(1), pp. 191-206.

Goel, T., Haftka, R. T., Shyy, W., & Queipo, N. V. (2007). 'Ensemble of surrogates'. Structural and Multidisciplinary Optimization **33**(3), pp. 199–216.

Halder, P., Rhee, S. H., & Samad, A. (2017). 'Numerical optimization of wells turbine for wave energy extraction'. International Journal of Naval Architecture and Ocean Engineering, **9**(1), pp. 11-24.

Harrison, M. E., Batten, W. M. J., Myers, L. E., & Bahaj, A. S. (2010). 'Comparison between CFD simulations and experiments for predicting the far wake of horizontal axis tidal turbines'. IET Renewable Power Generation **4**(6), pp. 613-627.

Huang, Z., Wang, C., Chen, J., & Tian, H. (2011). 'Optimal design of aeroengine turbine disc based on kriging surrogate models'. Computers and Structures **89**(1–2), pp. 27–37.

Huang, B., & Kanemoto, T. (2015). 'Multi-objective numerical optimization of the front blade pitch angle distribution in a counter-rotating type horizontal-axis tidal turbine'. Renewable Energy **81**, pp. 837-844.

Jeong, S., Murayama, M., & Yamamoto, K. (2012). 'Efficient optimization design method using kriging model'. Journal of Aircraft **42**(5), pp. 1375–1375.

Lawson, M. J., Li, Y., & Sale, D. C. (2011, June 19–24). 'Development and verification of a computational fluid dynamics model of a horizontal-axis tidal current turbine'. In ASME 2011 30th International Conference on Ocean, Offshore and Arctic Engineering, Rotterdam, The Netherlands, pp. 711-720.

Lee, J. H., Park, S., Kim, D. H., Rhee, S. H., & Kim, M. C. (2012). 'Computational methods for performance analysis of horizontal axis tidal stream turbines'. Applied Energy **98**, pp. 512-523.

Lophaven, S.N., Nielsen, H.B., Sondergaard, J. (2002). 'DACE: A matlab kriging toolbox'. Technical University of Denmark, Lyngby, Denmark.

Ma, D., Zhao, Y., Qiao, Y., & Li, G. (2015). 'Effects of relative thickness on aerodynamic characteristics of airfoil at a low reynolds number'. Chinese Journal of Aeronautics **28**(4), pp. 1003–1015.

Marten, D., Wendler, J., Pechlivanoglou, G., Nayeri, C. N., & Paschereit, C. O. (2013). 'Qblade: an open source tool for design and simulation of horizontal and vertical axis wind turbines'. International Journal of Emerging Technology and Advanced Engineering (IJETAE) **3**, pp.264-269.

Matheron, G. (1963). 'Principles of geostatistics'. Economic geology **58**(8), pp. 1246-1266.

O'Doherty, T., Mason-Jones, A., O'Doherty, D. M., Byrne, C. B., Owen, I., & Wang, Y. (2009, September 7-10). 'Experimental and computational analysis of a model horizontal axis tidal turbine'. In 8th European Wave and Tidal Energy Conference (EWTEC), Uppsala, Sweden.

Park, S., Park, S., Rhee, S. H., Lee, S. B., Choi, J. -E., & Kang, S. H. (2013). "Investigation on the wall function implementation for the prediction of ship resistance'. International Journal of Naval Architecture and Ocean Engineering, **5**, pp. 33-46.

Park, S., Park, S., & Rhee, S. H. (2016). 'Influence of blade deformation and yawed inflow on performance of a horizontal axis tidal stream turbine'. Renewable Energy, **92**, pp. 321-332.

Raza, W., & Kim, K. Y. (2008). 'Shape optimization of wire-wrapped fuel assembly using kriging metamodeling technique'. Nuclear Engineering and Design **238**(6), pp.1332-1341.

Sacks, J., Welch, W. J., Mitchell, T. J., & Wynn, H. P. (1989). 'Design and analysis of computer experiments'. Statistical science, pp. 409-423.

Samad, A., Kim, K. Y., Goel, T., Haftka, R. T., &Shyy, W. (2008). 'Multiple surrogate modeling for axial compressor blade shape optimization'. Journal of Propulsion and Power **24**(2), pp. 301-310.

Seo, J., Lee, S.-J., Choi, W.-S., Park, S.-T., & Rhee, S. H. (2016). 'Experimental study on kinetic energy conversion of horizontal axis tidal stream turbine'. Renewable Energy **97**, pp. 784-797.

Simpson, T. W., Mauery, T. M., Korte, J., & Mistree, F. (2001). 'Kriging models for global approximation in simulation-based

multidisciplinary design optimization'. AIAA Journal **39**(12), pp. 2233–2241.

Song, M., Kim, M. C., Do, I. R., Rhee, S. H., Lee, J. H., & Hyun, B. S. (2012). 'Numerical and experimental investigation on the performance of three newly designed 100 kW-class tidal current turbines'. International Journal of Naval Architecture and Ocean Engineering **4**(3), pp. 241-255.

Tahani, M., Babayan, N., Astaraei, F. R., & Moghadam, A. (2015). 'Multi objective optimization of horizontal axis tidal current turbines, using Meta heuristics algorithms'. Energy Conversion and Management **103**, pp. 487–498

Wang, H., Zhu, X., & Du, Z. (2010). 'Aerodynamic optimization for low pressure turbine exhaust hood using kriging surrogate model'. International Communications in Heat and Mass Transfer **37**(8), pp. 998–1003

DISCUSSION

Question from Jose Falcao De Campos

I would be interested in the reason for selecting the Tip speed ratio or TSR=3.5, with a relatively low power coefficient to focus the foil design optimization.

Authors' closure

The tip speed ratio or TSR=3.5 is the design tip speed ratio of the reference turbine. The power coefficient is maximum at the design TSR, and it drops drastically beyond the design TSR due to stall phenomenon.

The maximum power coefficient of the reference turbine at design TSR=3.5 is 26.2. Moreover, the value of the power coefficient of the reference turbine is less, hence the thickness parameters of the hydrofoil are optimized to improve the power coefficient of the turbine. The optimization significantly improved the power coefficient and off design performance of the turbine.